Asian Journal of Andrology (2024) 26, 535–543
www.asiaandro.com; https://journals.lww.com/ajandrology

Open Access

ORIGINAL ARTICLE

Prostate Disease

Safety of low-intensity extracorporeal shock wave therapy in prostate disorders: *in vitro* and *in vivo* evidence

Yi-Ran Wang[1,*], Bin Feng[2,*], Wen-Bo Qi[3], Yu-Wen Gong[1], Xiang-Bin Kong[1], Hui Cheng[4], Zhi-Long Dong[1], Jun-Qiang Tian[1], Zhi-Ping Wang[1]

Recent evidence suggests that low-intensity extracorporeal shock wave therapy (Li-ESWT) is a promising treatment for chronic prostatitis/chronic pelvic pain syndrome (CP/CPPS); however, its safety in pelvic organs, particularly prostate tissues and cells, remains unclear. The current study evaluates the risks of prostate cell damage or oncogenesis following the administration of Li-ESWT for prostatitis. To this end, a robust *in vitro* model (Cell Counting Kit-8 [CCK-8] assay, clone formation assay, cell scratch assay, lactate dehydrogenase [LDH] release assay, flow cytometry, and immunoblotting assay) was designed to examine the effects of Li-ESWT on cell proliferation, clonogenicity, migration, membrane integrity, and DNA damage. Exome sequencing of Li-ESWT-treated cells was performed to determine the risk of carcinogenesis. Furthermore, an *in vivo* rat model (n = 20) was employed to assess the effects of Li-ESWT on cancer biomarkers (carcinoembryonic antigen [CEA], Ki67, proliferating cell nuclear antigen [PCNA], and gamma-H2A histone family member X, phosphorylation of the H2AX Ser-139 [γ-H2AX]) in prostate tissue. Based on our findings, Li-ESWT promotes cellular growth and motility without inducing significant cell membrane or DNA damage or alterations. Genetic analyses did not demonstrate an increase in mutations, and no damage to prostate tissue or upregulation of cancer biomarkers was detected *in vivo*. This comprehensive *in vitro* and *in vivo* assessment confirms the safety of Li-ESWT in managing prostate disorders.

Asian Journal of Andrology (2024) **26**, 535–543; doi: 10.4103/aja202448; published online: 06 August 2024

Keywords: carcinogenesis; chronic pelvic pain syndrome; extracorporeal shock wave therapy; prostatitis; safety

INTRODUCTION

Extracorporeal shock wave therapy (ESWT), initially introduced as extracorporeal shock wave lithotripsy (ESWL) in 1980, has emerged as an innovative technical advancement for urologists to manage urinary stones.[1] Meanwhile, the application of low-intensity ESWT (Li-ESWT), a form of micro-energy medicine, harnesses low-energy sound waves to foster natural healing, improve blood circulation and tissue regeneration, and alleviate pain through neovascularization and stem cell recruitment among other mechanisms.[2] Beyond its initial urological applications, Li-ESWT has shown promise in treating myriad conditions, including erectile dysfunction,[3–5] chronic musculoskeletal pains, and notably, chronic prostatitis/chronic pelvic pain syndrome (CP/CPPS),[2,6,7] enhancing patients' quality of life since its initial application for CP/CPPS in 2008.[8–12] Indeed, Li-ESWT has demonstrated promising efficacy in treating various andrological disorders.[13–16] Our previous study provides insights into the effectiveness and mechanism of action of Li-ESWT in treating CPPS.[17] However, recent studies have yielded mixed results regarding the impact of Li-ESWT on male fertility. For example, while some researchers found no significant effect on sperm quality after a 3-month treatment period, others have detected a reduction in sperm production and reported instances of short-term urethral bleeding in rat models. These findings suggest that Li-ESWT may damage organs adjacent to the focal treatment area.[3,14,18]

Li-ESWT affects the whole prostate tissue during CP/CPPS treatment. Prostate epithelial cells are susceptible to an array of external and internal stimuli that may lead to detrimental outcomes such as DNA damage, cellular injury, and abnormal proliferation.[19] The development and advancement of prostate cancer is a consequence of intricate genetic and environmental interplay, including exposure to chemical agents, inflammatory conditions, and genetic susceptibilities.[20,21] These elements have the potential to kick-start the process of carcinogenesis by destabilizing cellular genetic material, whether directly or indirectly by disrupting DNA repair mechanisms.[19] Despite its widespread application in alleviating symptoms of CP/CPPS, the comprehensive biological impacts of Li-ESWT on prostate tissue and adjacent soft tissues remain partially understood.[22] While existing clinical trials have highlighted the therapeutic advantages of Li-ESWT, their

[1]Institute of Urology, Gansu Province Clinical Research Center for Urinary System Disease, The Second Hospital and Clinical Medical School, Lanzhou University, Lanzhou 730000, China; [2]Department of Urology, Gansu Provincial Hospital, Lanzhou 730000, China; [3]Department of Radiotherapy, First Affiliated Hospital of Zhengzhou University, Zhengzhou 450000, China; [4]Department of Urology, Gansu Provincial Second People's Hospital, Lanzhou 730000, China.
*These authors contributed equally to this work.
Correspondence: Dr. ZP Wang (erywzp@lzu.edu.cn)
Received: 10 November 2023; Accepted: 21 May 2024

limited duration and scope raise questions regarding the safety and carcinogenic potential of this therapy.[23–26] These gaps underscore the need for a detailed evaluation of the safety profile of Li-ESWT, particularly in the context of its potential to induce adverse biological effects or contribute to carcinogenesis in prostate tissues.[13]

Accordingly, in this study, we aimed to rigorously assess the short-term biological effects and safety of Li-ESWT through *in vitro* and *in vivo* models. This approach was designed to provide a thorough understanding of the mechanical and biological effects of Li-ESWT on prostate disorders, contributing valuable insights regarding its safety in treating CP/CPPS.

MATERIALS AND METHODS

Experimental design principles

To rigorously assess the safety of Li-ESWT in CP/CPPS, we implemented a multifaceted approach combining *in vitro* and *in vivo* models. Our innovative Li-ESWT *in vitro* model ensured uniform mechanical force distribution, overcoming a common research limitation and allowing for precise measurements (**Figure 1a** and **1b**). We selected the following cell lines to represent potentially affected pelvic organs in patients with CP/CPPS: RWPE-1 (prostate epithelial), DU145 (prostate cancer), SV-HUC-1 (bladder epithelial), and NCM460 (intestinal epithelial). Using these cell lines, we evaluated the impact of Li-ESWT on cell viability, proliferation, and DNA integrity to address concerns regarding potential tissue damage or tumorigenic effects.

RWPE-1 cells are derived from normal human prostate epithelium and are frequently used to study prostate cell biology and responses to treatments, given their representative characteristics of prostate epithelial cells. The use of RWPE-1 cells in prior studies to examine cellular mechanisms and therapeutic impacts on prostate health underscores their suitability for investigating the effects of Li-ESWT. Hence, the utilization of RWPE-1 cells ensured that our results were comparable to existing studies on prostate treatments. Furthermore, our experimental protocol mirrored clinical treatment conditions, maximizing the relevance and translational impact of our findings.

Li-ESWT equipment

Prototype shock wave therapy equipment is shown in **Figure 1c**, provided by Shenzhen Wellcome Company (Shenzhen, China). This equipment comprises a piezoelectric probe that produces linearly focused extracorporeal shock waves. Moreover, it offers adjustable parameters, allowing for fine-tuning of shock wave intensity across five levels (G1–G5) and frequency settings ranging from 1 Hz to 3 Hz.

Cell lines and cell culture

Human RWPE-1 cells were procured from Hunan Fenghui Biotechnology (Changsha, China), while DU145 and SV-HUC-1 cell lines were obtained from the Cell Bank of the Chinese Academy of Sciences (Shanghai, China). The NCM460 cell line was provided by the Dr. Hao Chen's Laboratory (Key Laboratory of the Digestive System Tumors of Gansu Province, Lanzhou University Second Hospital, Lanzhou, China). Short tandem repeat (STR) genotyping confirmed the authenticity of the cell lines. RWPE-1 cells were cultured in Gibco Keratinocyte-SFM (1×; Thermo Fisher Scientific, Waltham, MA, USA), supplemented with 50 mg ml^{-1} bovine pituitary extract (BPE), 5 ng ml^{-1} epidermal growth factor, and 1% antibiotic mixture (100 U ml^{-1} penicillin, 100 mg ml^{-1} streptomycin, and 0.25 mg ml^{-1} amphotericin B). DU145, SV-HUC-1, and NCM460 cells were cultured in minimum essential medium (MEM; L550KJ; BasalMedia, Shanghai, China), Ham's F-12K medium (L450KJ; BasalMedia), and Dulbecco's modified Eagle's medium (DMEM; L110KJ; BasalMedia), respectively, supplemented with 10% fetal bovine serum (FBS) and 1% antibiotic mixture containing 100 U ml^{-1} penicillin and 100 mg ml^{-1} streptomycin. All cells were incubated at 37°C under 5% CO_2 and 95% humidity.

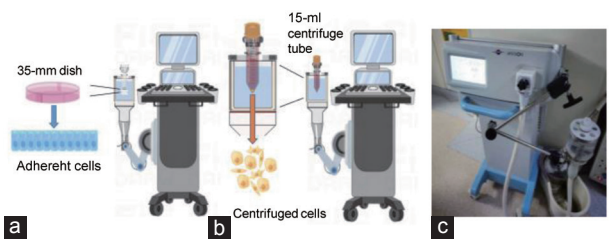

Figure 1: Establishment of the Li-ESWT *in vitro* model and measurement of its physical parameters. (**a**) Schematic diagram of the Li-ESWT adherent cell *in vitro* model. (**b**) Schematic diagram of the Li-ESWT nonadherent cell *in vitro* model. (**c**) Li-ESWT device used in this study. Li-ESWT: low-intensity extracorporeal shock wave therapy.

Li-ESWT in vitro experimental protocol

For the adherent cell Li-ESWT model, an appropriate number of cells were seeded in 35-mm culture dishes 24 h before assaying adherent cells in the Li-ESWT model. Subsequently, the culture dishes were directly introduced into the Li-ESWT model for intervention.

For the nonadherent cell Li-ESWT model, a specific quantity of adherent cells was seeded into a 100-mm culture dish and subsequently incubated at 37°C under 5% CO_2 and 95% humidity. Subsequently, the cells underwent digestion and were resuspended in complete culture medium in a 15-ml centrifuge tube. The suspension was then centrifuged (3K15; Sigma-Aldrich, St. Louis, MO, USA) at 200*g* for 3 min; centrifuged cells were resuspended for Li-ESWT. All experiments were performed at a consistent frequency of 3 Hz, meaning that 500 pulses took approximately 3 min and 1000 pulses took approximately 6 min. Cell fusion efficiency was monitored, ensuring that it reached 80%–90% before initiating Li-ESWT.

Cell proliferation assay

An appropriate number of cells, treated with 500 pulses or 1000 pulses of different Li-ESWT levels, were seeded into a 96-well plate and incubated at 37°C for 24 h or 48 h in the presence of 5% CO_2. Following incubation, 5% Cell Counting Kit-8 (CCK-8) reagent was added to each well, and the plates were further incubated at 37°C in the dark for 30 min. Subsequently, the absorbance was measured at 450 nm using a spectrophotometer (Infinite M200 Pro; TECAN, Shanghai, China).

Cell clone formation assay

Cells subjected to 1000 pulses of different Li-ESWT levels were resuspended in complete culture medium and quantified. For the cell clone formation experiment, approximately 1000 cells were seeded into each well of a 6-well plate. Subsequently, the cells were incubated at 37°C for approximately 2 weeks in the presence of 5% CO_2. After incubation, the cells were gently washed with phosphate-buffered saline (PBS) and fixed with 4% paraformaldehyde solution at room temperature for 10 min. Following fixation, cells were rinsed twice with PBS and stained with 1% crystal violet solution for 10 min. Finally, the cells were photographed against a white background.

Cell scratch assay

To assess cell migration, RWPE-1 and DU145 cells were treated with 1000 pulses of Li-ESWT at the G2 and G3 phases, using a nonadherent *in vitro* model. Following Li-ESWT, cells were resuspended in complete culture medium and counted. Cells were seeded in 6-well plates at a

density of approximately 400 000 cells per well and incubated at 37°C for 24 h to establish a monolayer. Subsequently, scratches (wounds) were created across the cell monolayer. Detached cells and debris were carefully removed. RWPE-1 cells were supplemented with complete culture medium, whereas DU145 cells were supplemented with serum-free medium. These plates were incubated at 37°C for 24 h and 48 h in the presence of 5% CO_2. Images were captured using phase-contrast microscopy (AxioVert.A1; Carl Zeiss AG, Oberkochen, Germany) to monitor cell migration into the scratched areas.

Lactate dehydrogenase (LDH) release assay

To examine cytotoxicity following 1000 pulses with various Li-ESWT levels, an appropriate number of cells were seeded into a 96-well plate. The cells were incubated at 37°C for 24 h in the presence of 5% CO_2. Following incubation, the supernatant was collected, and the LDH concentration was measured using the LDH release assay kit (Beyotime, Shanghai, China) according to the manufacturer's instructions.

Flow cytometry

Flow cytometry was used to detect cell membrane damage. Briefly, resuspended cells treated with 1000 pulses of Li-ESWT were incubated with Annexin V-mCherry reagent (Beyotime) at 37°C for 30 min in the dark. Subsequently, the cells were washed twice with PBS and subjected to flow cytometric analysis.

To assess apoptosis, ESW-treated cells were resuspended, and an appropriate number of cells were seeded into a 6-well plate. After 24 h and 48 h of incubation, Annexin V-mCherry/SYTOX Green apoptosis detection reagent (Beyotime) was added according to the manufacturer's protocol. The cells were analyzed using a flow cytometer (Beckman Life Sciences, Shanghai, China). All data were analyzed using CytExpert 2.5 software (Beckman).

Immunoblotting assay

In the nonadherent *in vitro* cell model, RWPE-1 cells were treated with 1000 pulses of Li-ESWT at the G1–G5 levels. Immediately after treatment, the cells were centrifuged, and proteins were extracted for immunoblot analysis. Proteins were extracted via freeze-thaw lysis at −80°C using radioimmunoprecipitation assay (RIPA) buffer (150 mmol l^{-1} NaCl, 1% [*v*/*v*] NP-40, 0.5% [*w*/*v*] sodium deoxycholate, 0.1% [*w*/*v*] sodium dodecyl sulfate [SDS], and 25 mmol l^{-1} Tris), followed by the addition of a protease and phosphatase inhibitor cocktail (P002; NCMbio, Suzhou, China). The protein content was quantified using the bicinchoninic acid (BCA) method (PC0020; Solarbio, Beijing, China). Subsequently, 5–10 mg of protein was combined with 5× Laemmli buffer (50 mmol l^{-1} Tris-HCl pH 6.8, 4% [*w*/*v*] SDS, 10% [*v*/*v*] glycerol, 0.1% [*w*/*v*] bromophenol blue [1610404; Bio-Rad, Shanghai, China], and 2% [*v*/*v*] β-mercaptoethanol [1610710; Bio-Rad]) to achieve a final 1× concentration and was heated to 95°C.

The proteins were separated through SDS-polyacrylamide gel electrophoresis and transferred onto polyvinylidene difluoride membranes. The membranes were washed twice with TBST (20 mmol l^{-1} Tris, 150 mmol l^{-1} NaCl, and 0.1% [*w*/*v*] Tween 20) and blocked for 1 h at room temperature with 5% milk TBST buffer on an orbital shaker. Subsequently, the membranes were incubated with primary antibodies at 4°C for 12 h and washed thrice with TBST. The membranes were probed with a horseradish peroxidase-conjugated secondary antibody at room temperature for 1 h. The membranes were washed with TBST thrice. Immunoblots were visualized using autoradiography. The following antibodies were used: phospho-H2A histone family member X (H2AX; phosphorylation of the H2AX Ser-139 [γ-H2AX];9718; Cell Signaling Technology, Danvers, MA, USA), H2AX (10856-1-AP; Proteintech, Wuhan, China), and poly (ADP-ribose) polymerase 1 (PARP1; 80174-1-RR; Proteintech).

Exome sequencing

Furthermore, genomic DNA was fragmented using NEBNext dsDNA Fragmentase (NEB Inc., Ipswich, MA, USA), followed by DNA end repair. End-repaired DNA fragments were dA-tailed and ligated using the NEBNext adaptor (NEB Inc., Shanghai, China). Subsequently, biotinylated RNA library baits and magnetic beads were combined with the barcoded library for targeted region selection using a SureSelect Human All Exon V6 Kit (Agilent Technologies, Palo Alto, CA, USA). The captured sequences were amplified by 150 bp paired-end sequencing using an Illumina X-ten system (Illumina, San Diego, CA, USA).

The datasets generated and analyzed in the present study are available from the corresponding author upon reasonable request. The exome sequencing raw data generated in this study have been deposited in the National Center for Biotechnology Information's database under accession code PRJNA1023701.

Animal experimental details and ethical compliance

This research was performed at the Institute of Urology, Lanzhou University Second Hospital (Lanzhou, China), from May to July 2020, and adhered strictly to the highest ethical standards in animal experimentation. The study received ethical clearance from the Animal Experiment Ethics Committee of Lanzhou University Second Hospital (Approval No. D2019-177). Our protocols for animal handling and experimentation were designed to align with the "Guidelines for the Care and Use of Laboratory Animals" (NIH publication No. 85–23, National Academies Press, Washington, DC, USA, revised 1996).

A total of twenty male Sprague-Dawley rats (2 months old, 180–220 g body weight) were sourced from the Lanzhou Veterinary Research Institute, Chinese Academy of Agricultural Sciences (Lanzhou, China). The rats were maintained in a specific pathogen-free setting under controlled environmental conditions of 23°C ± 2°C and 55% ± 5% humidity. Before initiating the experimental activities, all animals were subjected to a week-long acclimatization period, during which they had unrestricted access to food and water. This preparatory phase was crucial for ensuring their optimal well-being and minimizing potential stress.

Li-ESWT in vivo experimental protocol

Twenty Sprague-Dawley rats were divided into the sham and Li-ESWT groups (n = 10 per group). In the Li-ESWT group, Li-ESWT was performed thrice weekly for 4 weeks, with totally 12 sessions. During the Li-ESWT procedure, we anesthetized the rat with 1% sodium pentobarbital via intraperitoneal injection, shaved the abdominal hair, and secured the rat in a supine position on the operating table. We then applied a coupling agent to the shock wave generator probe and placed it against the pubic area for intervention. Each Li-ESWT session comprised 2000 pulses at the G5 level, *i.e.*, the processing time of each Li-ESWT was approximately 12 min. The sham group was anesthetized but received no other treatment.

On day 28 of modeling, rats were euthanized under anesthesia. Prostates were harvested via midline abdominal incision, revealing bright red, firm tissue adjacent to the bladder. Excised prostates were rinsed with PBS, and excess fat was removed. One lobe was snap-frozen at −80°C for future analysis, while the other was formalin-fixed, paraffin-embedded, and sectioned at 4 μm for immunohistochemical staining.

Immunohistochemistry

Carcinoembryonic antigen (CEA), Ki67, proliferating cell nuclear antigen (PCNA), and γ-H2AX were selected as the immunohistochemical markers. Tissue microarray samples were cut into 4 μm-thick serial sections, placed in an oven at 67°C for 30 min, and dewaxed in xylene and alcohol. Subsequently, the tissue samples were treated with TE buffer (10 mmol l^{-1} Tris, 1 mmol l^{-1} ethylenediaminetetraacetic acid [EDTA], pH 9.3) at 98°C for 30 min. To eliminate endogenous peroxidase activity, the tissue samples were immersed in 3% H_2O_2. The samples were then incubated with primary antibodies in PBS + Tween 20 (PBST) containing 3 mg ml^{-1} goat globulin (Sigma-Aldrich) for 60 min at room temperature (25°C). Subsequently, the samples were incubated with an anti-mouse/rabbit secondary antibody (Envision Plus, Dako, Shanghai, China) for 30 min at room temperature (approximately 25°C). Finally, chromogenic agent 3,3′-diaminobenzidine (Dako) was used to stain the tissue samples for visualization.

Statistical analyses

GraphPad Prism 8 (GraphPad Software Inc., San Diego, CA, USA) was used for data analysis. Student's *t*-test was used to compare data between the two groups. Statistical significance was set at $P < 0.05$.

RESULTS

Establishment of the Li-ESWT in vitro model and physical parameter measurement

The first *in situ* model was primarily designed for adherent cells (vector diagram is showed in **Figure 1a**, and actual photo is showed in **Supplementary Figure 1a**), where a 35-mm culture dish was placed in the water reservoir of the Li-ESWT device probe, allowing stable mechanical stimulation of the cells. The second model was designed for nonadherent cells, including postdigestion adherent cells (vector diagram is showed in **Figure 1b**, and actual photo is showed in **Supplementary Figure 1b**), in which a 15-ml plastic centrifuge tube was positioned in the water reservoir of the ESW device probe to achieve stable mechanical stimulation of the cells. The physical parameters of the mechanical stimulation (G1–G5), as experienced by cells in culture dishes and tubes, were determined after establishing the Li-ESWT *in vitro* model (**Supplementary Table 1**). We observed that Li-ESWT-induced mechanical stimulation within the centrifuge tube did not exhibit a progressive increase from G1 to G5. Notably, minimal mechanical stimulation was observed at the G2 level, with the intensity at G1 comparable to that observed between G4 and G5.

Effect of Li-ESWT on in vitro cell biology

Li-ESWT-treated RWPE-1 cells exhibited distinct responses within the nonadherent cell model. Li-ESWT exceeding 200 pulses caused a cavitation effect, leading to cell detachment at the treatment focal point, making further experiments with adherent cells impractical (**Supplementary Figure 1c**).[27] In the *in vitro* adherent cell model, Li-ESWT-treated RWPE-1 cells showed no significant changes in proliferation at 24 h or 48 h posttreatment, as evidenced by the CCK-8 assay results (**Supplementary Figure 1d**).

Consequently, we shifted our focus to the nonadherent cell model, which tolerated over 2000 Li-ESWT pulses without adverse effects. Cell proliferation significantly increased at 48 h after 500 pulses of Li-ESWT at G1–G5 ($P<0.05$), whereas there was no significant difference in cell proliferation after 500 pulses of Li-ESWT at G1–G5 for 24 h ($P>0.05$; **Figure 2a**). Meanwhile, cell proliferation was significantly increased at 24 h (both $P<0.05$) and 48 h (both $P<0.001$) after 1000 pulses at G1 and G2 (**Figure 2b**). However, none of the Li-ESWT strengths applied reduced RWPE-1 cell proliferation. According to the CCK-8 assay results for the SV-HUC-1 ($P<0.05$; **Figure 2c**) and NCM460 ($P<0.05$; **Figure 2d**) cell lines, both showed increased proliferation at the G1 and G2 levels, with no decreasing tendency observed.

The CCK-8 assay results revealed no significant differences in the proliferation of adherent cells; this was attributed to the uneven mechanical stimulation caused by cavitation effects in adherent cell models. Accordingly, we selected the *in vitro* nonadherent cell model for subsequent experiments. RWPE-1 cells were treated with 1000 pulses of Li-ESWT, cultured for 2 weeks, and stained with 1% crystal violet solution. Analysis of cells using ImageJ software indicated no statistical difference in the number of clones formed in the G2 and G3 groups compared with the other groups (**Figure 2e** and **2f**).

Effect of Li-ESWT on prostate epithelial and cancer cell migration in vitro

Based on the scratch experiment results, there were no significant differences in the RWPE-1 cell migration distance among the G2, G3, and sham groups at 24 h and 48 h (**Figure 2g**). Conversely, DU145 cells in the G2 and G3 groups exhibited decreased migration compared with cells in the sham group at 24 h, with the G2 group exhibiting increased migration at 48 h (**Figure 2h**).

Effect of Li-ESWT on the plasma membrane integrity of prostate epithelial cells in vitro

No significant differences were observed between the G1 and G3 groups compared with the control group. The G5 group exhibited an approximately 20% increase, albeit statistically insignificant ($P>0.05$; **Figure 3a**). Following treatment of RWPE-1 cells with Li-ESWT at the G5 level for 24 h, a significant increase in LDH release was observed starting from the 1000-pulse group, with an average increase of approximately 15%–20% (both $P<0.05$; **Figure 3b**). Treatment with Li-ESWT at G2 and G3 levels did not increase Annexin V levels in the cytoplasmic membrane, although a slight decrease was observed (**Figure 3c**). Moreover, no significant differences in apoptotic levels were detected between the Li-ESWT treatment groups and the sham group (**Figure 3d** and **3e**).

Effect of Li-ESWT on DNA damage in the in vitro prostate epithelial cell model

Next, we examined whether Li-ESWT induced any DNA damage in RWPE-1 cells *in vitro*. PARP-1 and H2AX were selected as markers for DNA damage, given that both are essential components in DNA damage repair. Western blot results revealed that the γ-H2AX levels did not differ significantly between the G1–G5 and sham groups. Additionally, no western blot bands indicating PARP1 cleavage were observed in the G1–G5 groups (**Figure 4a**). Moreover, the levels of γ-H2AX and PARP1 cleavage proteins in different pulses G2 level did not significantly differ from those in the sham group (**Figure 4b**).

Effect of Li-ESWT on whole-exome sequencing in a prostate epithelial cell model in vitro

To determine the impact of various Li-ESWT strengths on cells at the gene level, RWPE-1 cells were treated with 1000 pulses of Li-ESWT at G2, G3, G4, and G5 levels, with each group receiving a total of ten treatments (**Figure 5a**). Given that changes in cell malignancy are closely related to altered morphology, we monitored the cells for morphological changes according to a previously described method.[28] Microscopic examination (20×) after 24 h of culture revealed no apparent morphological changes in any of the four ESW treatment groups compared with the sham group (**Supplementary Figure 1e**).

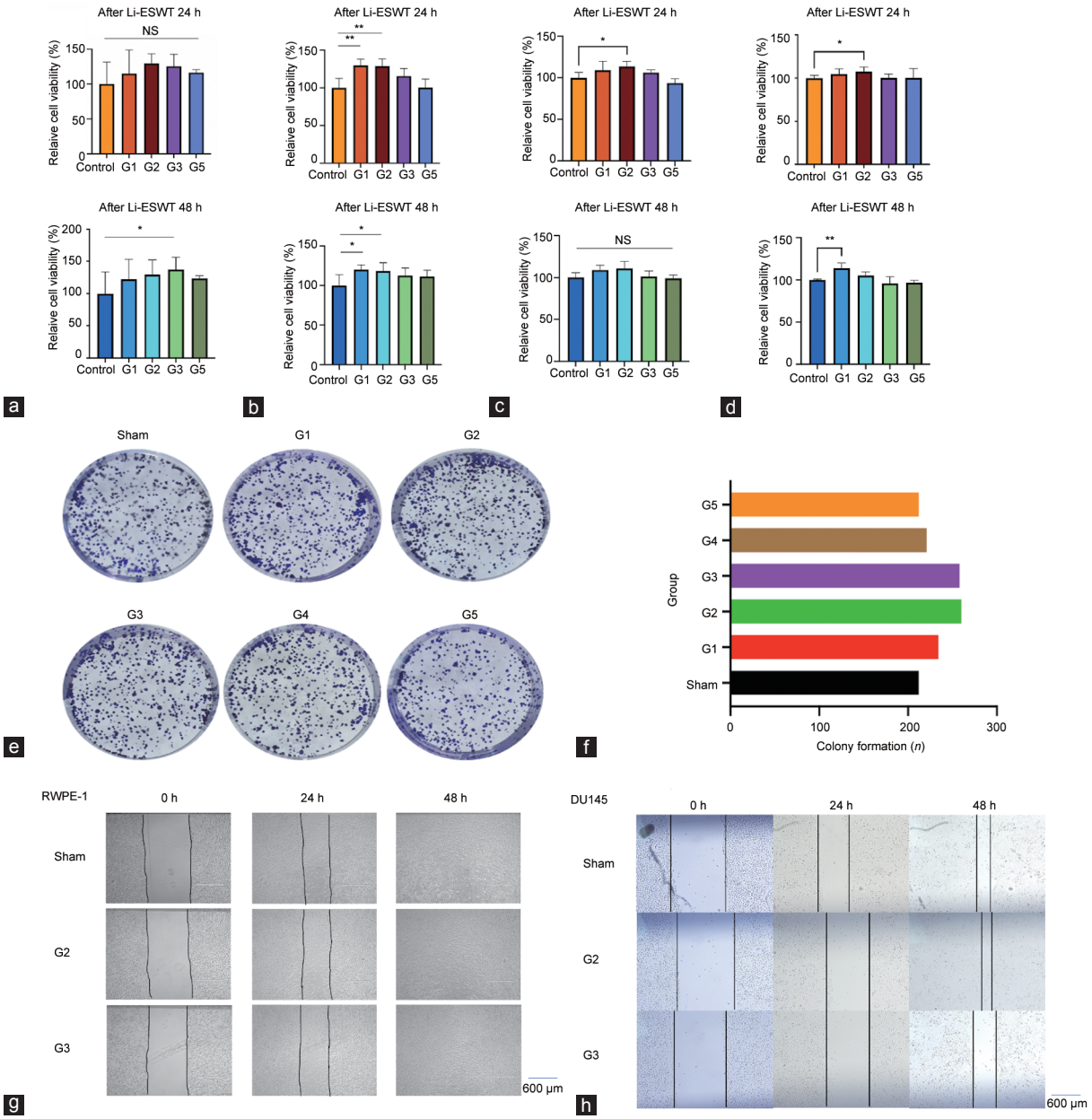

Figure 2: Effect of Li-ESWT on prostate epithelial cell proliferation, colony formation, and migration in the *in vitro* model. (**a**) CCK-8 assay results of the nonadherent RWPE-1 *in vitro* model cells after exposure to 500 pulses of Li-ESWT at different levels. (**b**) CCK-8 assay results of the nonadherent RWPE-1 *in vitro* model cells after exposure to 1000 pulses of Li-ESWT at different levels. (**c**) CCK-8 assay results of the nonadherent SV-HUC-1 *in vitro* model cells after exposure to 1000 pulses of Li-ESWT at different levels. (**d**) CCK-8 assay results of nonadherent NCM460 *in vitro* model cells after exposure to 1000 pulses of Li-ESWT. (**e**) Colony formation of RWPE-1 cells after exposure to different 1000 pulses of Li-ESWT levels in the nonadherent *in vitro* cell model. (**f**) Histogram of clone formation number. Representative images of (**g**) RWPE-1 and (**h**) DU145 cell migration after exposure to different levels of Li-ESWT. Scale bars=600 μm. Data were evaluated using Student's *t*-test and are presented as mean ± s.d. $^{**}P < 0.01$, $^{*}P < 0.05$, the indicated value compared that in the control group. G1–G5: Li-ESWT energy levels 1–5. CCK-8: Cell Counting Kit-8; Li-ESWT: low-intensity extracorporeal shock wave; s.d.: standard deviation; NS: not statistically significant.

We combined all Li-ESWT-treated cells into the Li-ESWT group and used the sham group as a control. DNA was extracted from both groups for whole-exome sequencing, with three biological replicates per group. Analysis revealed no significant differences in the number of single-nucleotide polymorphisms (SNPs) or insertion–deletion mutations (InDels) between the Li-ESWT and control groups (**Supplementary Table 2**). The genomic locations and types of SNPs in the Li-ESWT group did not differ significantly from those in the control group (**Figure 5b**). Similarly, the types of InDels and the information in the coding regions did not differ significantly between the Li-ESWT and control groups (**Figure 5b**). No significant increase in structural variations (SVs), *i.e.*, large-scale modifications in the genome, was detected in the treatment groups compared with the control group across various SV categories (**Figure 5c**).

Carcinogenic effects of Li-ESWT on in vivo rat prostate model

After completing all Li-ESWT sessions, prostate tissues from the sham and Li-ESWT groups were examined, with no apparent signs of damage

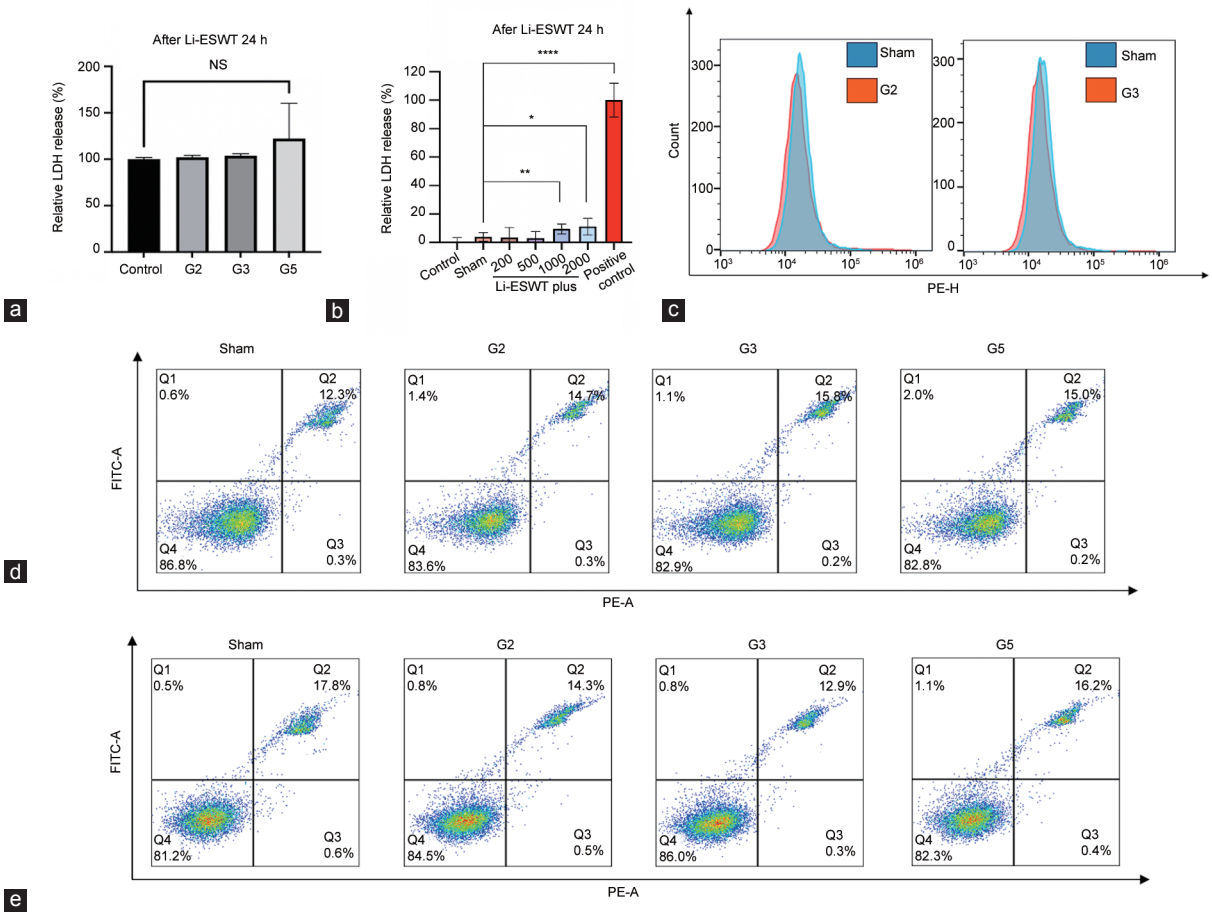

Figure 3: Li-ESWT does not disrupt the plasma membrane integrity in the prostate epithelial cell *in vitro* model. (**a**) LDH release from RWPE-1 cells after exposure to 1000 Li-ESWT pulses at different levels. (**b**) LDH release from RWPE-1 cells after exposure to the G5 level using 200–2000 Li-ESWT pulses. Data were evaluated using Student's *t*-test and are presented as mean ± s.d.. $^{****}P < 0.0001$, $^{**}P < 0.01$, $^{*}P < 0.05$, the indicated value compared that in the control group. (**c**) Flow cytometry data of RWPE-1 cells after exposure to 1000 pulses of Li-ESWT at the G2 (left) and G3 (right) levels. (**d**) Flow cytometry data of RWPE-1 cells after exposure to 1000 pulses of Li-ESWT at G2, G3, and G5 levels and cultured for 2 h. (**e**) Flow cytometry data of RWPE-1 cells after exposure to 1000 pulses of Li-ESWT at G2, G3, and G5 levels and cultured for 24 h. G2, G3 and G5: Li-ESWT energy levels 2, 3 and 5, respectively. LDH: lactate dehydrogenase; Li-ESWT: low-intensity extracorporeal shock wave; s.d.: standard deviation; NS: not statistically significant; PE-H: phycoerythrin height; FITC-A: fluorescein area; PE-A: phycoerythrin area.

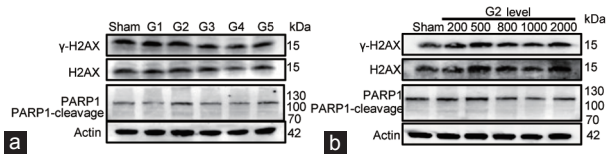

Figure 4: Li-ESWT does not induce DNA damage in the prostate epithelial cell *in vitro* model. (**a**) Western blot of RWPE-1 cells exposed to 1000 Li-ESWT pulses at G1, G2, G3, G4, and G5 levels. (**b**) Western blot of RWPE-1 cells exposed to different pulses of Li-ESWT at the G2 level. G1–G5: Li-ESWT energy levels 1–5. Li-ESWT: low-intensity extracorporeal shock wave; H2AX: H2A histone family member X; γ-H2AX: phosphorylation the H2AX Ser-139; PARP1: poly (ADP-ribose) polymerase 1.

identified in either group (**Figure 6a** and **6b**). Compared to the sham group, the staining intensities of all three carcinogenic markers did not differ significantly in the Li-ESWT group; however, slight decreases were observed in select cases (**Figure 6c**).

DISCUSSION

Li-ESWT represents a novel therapeutic approach for managing CP/CPPS, yet its potential side effects and carcinogenic risks to prostate tissue are not well understood. In our research, we have developed improved *in vitro* and *in vivo* models to thoroughly evaluate the effects of Li-ESWT on cellular biology and its carcinogenic potential, with a particular focus on safety in prostate tissue treatment.

The transformation of prostate epithelial cells into cancerous cells involves complex molecular and genetic mechanisms.[29,30] Evidence-based medicine has identified key risk factors, including diet, androgen exposure, obesity, and activation of the phosphatidylinositol-4,5-bisphosphate 3-kinase/protein kinase B (PI3K/AKT) pathway, which are crucial for the malignant transformation of prostate epithelial cells.[31,32] Studies on the carcinogenicity of prostate cancer have revealed that exposure to specific agents, such as N-nitroso-N-methylurea (NMU), cadmium, and radiation, can significantly promote the neoplastic transformation of prostate epithelial cells. These findings underscore the relationship between malignant cellular changes and alterations in wound healing processes as well as cellular morphology, suggesting that these factors likely contribute to the development of prostate cancer.[28,33–35]

Basic research on physical treatment modalities has historically placed limited emphasis on their potential carcinogenic effects.

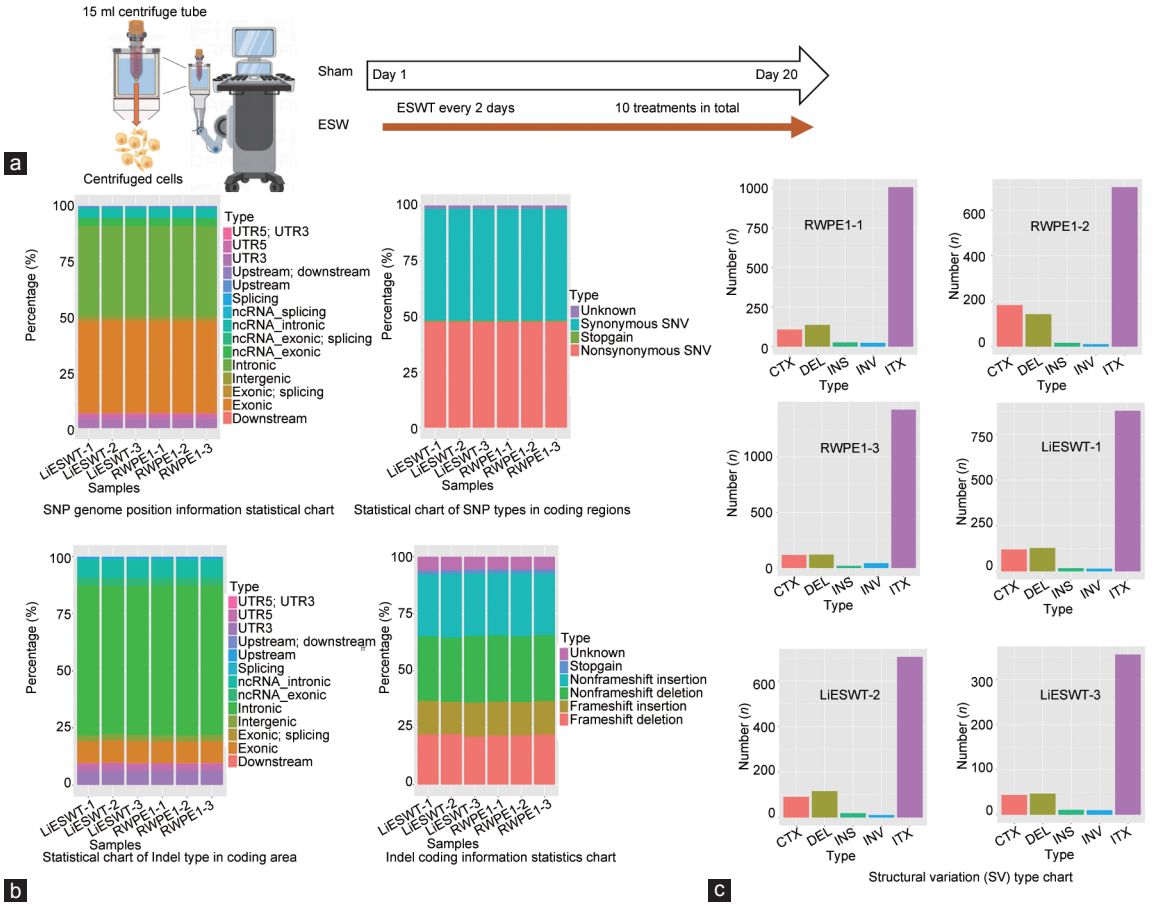

Figure 5: Li-ESWT does not induce hereditary changes in the prostate epithelial cell *in vitro* model. (**a**) Schematic diagram of the RWPE-1 *in vitro* cell model and sham group treated with Li-ESWT. (**b**) SNP and Indel mutations results, and (**c**) SV results of the Li-ESWT (ESW group) *vs* the RWPE-1 (sham group) , respectively. DEL: deletion; INS: insertion; INV: inversion; ITX: intrachromosomal translocation; CTX: interchromosomal translocation; ESW: extracorporeal shock wave; Li-ESWT: low-intensity extracorporeal shock wave; SV: structural variation; SNP: single nucleotide polymorphism; UTR: untranslated region; ncRNA: non-coding RNA.

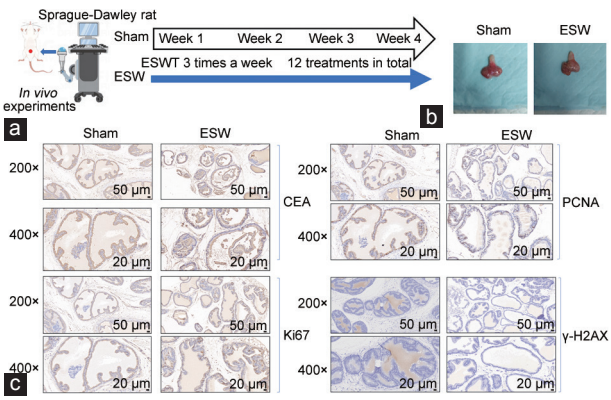

Figure 6: Li-ESWT does not induce carcinogenicity in the rat prostate *in vivo* model. (**a**) Schematic diagram of the *in vivo* model of Sprague-Dawley rats treated with Li-ESWT. (**b**) Representative images of the rat prostate of the sham and ESW groups. (**c**) Representative immunochemistry images of the sham and ESW groups (Li-ESWT). CEA: carcinoembryonic antigen; PCNA: proliferating cell nuclear antigen; γ-H2AX: gamma-H2A histone family member X, phosphorylation of the H2AX Ser-139; ESW: extracorporeal shock wave; Li-ESWT: low-intensity extracorporeal shock wave.

Accordingly, the current study's Li-ESWT model was developed within the existing research context.[28,33–35] Our findings indicate that prostate epithelial cells subjected to Li-ESWT do not exhibit characteristics indicative of malignant transformation, which lends credence to the safety profile of this treatment modality.

Interestingly, the most effective Li-ESWT settings for promoting cell proliferation, clone formation, and migration were at the lower G2 energy level. This is consistent with the conclusion of existing studies that report a certain effective range of trigger points for mechanotransduction effects.[13,36,37] This suggests that lesser mechanical damage through moderated energy settings might optimize biological effects. In fact, the observed biological effects in nonadherent cell models but not in adherent cells can be explained by differences in mechanical force distribution (**Figure 2a–2d**). In adherent cell models, typically cultured on flat surfaces, the mechanical forces are evenly distributed. In contrast, nonadherent models experience a more varied distribution of forces. This inconsistency may prevent cells in nonadherent models from uniformly receiving and responding to mechanical forces across different energy levels. Indeed, we confirmed that the "indirect effects" of shock waves, biomechanical rather than direct impacts, are likely the primary influencers of cell proliferation. That is, Li-ESWT at the G2 level maximized biological effects by inducing a balance of direct mechanical stimulation and milder "calcium wave" signals, enhancing cell proliferation and migration while reducing stress responses (unpublished data). This nuanced

understanding highlights how specific energy settings can subtly influence therapeutic outcomes in cellular environments.

The complex interplay between genetic and environmental factors, including free radicals and compromised DNA repair, encompasses the carcinogenic potential that can lead to cancer.[38–41] Based on previously reported results,[36,42,43] we posit that, in the absence of adverse effects, the angiogenic and proliferative responses induced by Li-ESWT within clinical treatment parameters are unlikely to contribute to the development of prostate tumors or other pathologies. Hence, this study expands beyond the discussion of the mechano-biological effects of Li-ESWT in the context of prostate cancer development. Our annexin V[44] results indicated that Li-EWST did not disrupt the cell membrane, indirectly implying that it also does not induce substantial sonoporation effects in cells, consistent with the findings of Takahashi *et al*.[36] This was further supported by the fact that the abundance of DNA damage, a key indicator for assessing potential carcinogenicity,[45] markers (γ-H2AX and PARP-1) did not increase in cells with higher energy levels or number of Li-ESWT treatments. Exome sequencing data analysis further revealed that genetic variations in the Li-ESWT treatment group (including SNPs, InDels, and SVs) did not differ significantly from the control group. Cumulatively, these findings suggest that Li-ESWT has minimal capacity to inflict cell damage through directly mechanical stimulation or alter the genetic makeup of cells *in vitro*.

Consistent with the parameters used in our concurrent clinical trials, we applied the G5 level and 2000 impulses of Li-ESWT to our *in vivo* rat model. This approach supports the hypothesis that higher energy levels (G5) in treating CPPS may lead to more favorable outcomes than lower levels (G2) because the pelvic region around the prostate can absorb considerable energy, leading to a significant reduction in the actual impact force on the prostate tissue.[46] Following the Li-ESWT treatment, the prostates of the animals were examined, and no signs of congestion or swelling were observed. Moreover, the staining intensity of CEA, Ki67, and PCNA (established markers of abnormal cell proliferation[47]) was uniform across the treated and control groups, indicating that clinical-grade Li-ESWT did not induce cell proliferation or cause cell damage *in vivo*. These results make a substantial contribution toward confirming the safety and noncarcinogenic properties of Li-ESWT, providing biological evidence that supports its potential as a safe treatment option for prostate disorders.

While the effects of Li-ESWT on cell biology have been well established,[48–50] safety studies are rare. This study provides innovative contributions to assessing the safety of Li-ESWT for treating prostate disorders. Moreover, our findings provide crucial insights that could guide further clinical trials of physical treatment modalities (*e.g.*, Li-ESWT) for prostate-related conditions, ensuring that safety and carcinogenicity concerns are adequately addressed. We believe that these models also offer a platform for further exploring the mechanisms of action employed by Li-ESWT in various cell processes and pathways.

Our research findings align with recent clinical trial results, suggesting that there are no notable short-term (within 1 year) clinical side effects observed following Li-ESWT treatment for patients with CP/CPPS.[23,25,26,51–53] Nevertheless, this study had certain limitations. First, besides carcinogenicity, our study did not thoroughly investigate other safety concerns that may arise from the use of Li-ESWT for prostate disease treatment. For instance, the prostate plays a crucial role in the male reproductive system, with prostate fluid as a major constituent of semen.[54] Our research did not examine whether Li-ESWT influences the prostate's ability to produce prostatic fluid throughout the treatment period, potentially impacting semen quality. Second, in formulating the carcinogenicity experiment for Li-ESWT, we singularly concentrated on whether mechanical stimulation leads to DNA damage in cells following short-term and long-term interventions, instigating genetic mutations and precipitating carcinogenesis. However, previous research has indicated that Li-ESWT can elicit other biological responses, such as angiogenesis and integrin signaling.[55] The question remains as to whether these "mild" biological effects, induced by "intense" mechanical stimulation, bear implications for the prostate after repeated applications or if they can engender side effects or carcinogenicity in other organs. Hence, future research should focus on long-term clinical data to thoroughly assess the mechanical induction effect of Li-ESWT, with the ultimate goal of fully reducing its clinical safety risks. Third, although this study sought to determine if Li-ESWT's mechanical stimulation causes DNA damage and gene mutations, it was limited by the use of basic *in vitro* and *in vivo* models that may not fully represent clinical conditions. This limitation suggests that the resulting safety data may not be entirely reflective of real-world clinical applications. To enhance the reliability of our findings, we increased the sample size and ensured a more diverse representation. Currently, our team is engaged in prospective clinical trials of Li-ESWT for CPPS treatment, with a particular focus on gathering long-term follow-up data to assess the therapy's sustained effects. We are committed to addressing the limitations of this study in our forthcoming research to provide a more comprehensive understanding of Li-ESWT's safety and efficacy.

CONCLUSION

Therapeutic interventions that result in cellular damage can induce genetic mutations and initiate abnormal cell proliferation, which may ultimately result in cancer. In the present study, we employed *in vitro* and *in vivo* models to delve into the biological impacts of Li-ESWT on cells, revealing that Li-ESWT does not elicit cellular damage. These findings provide robust evidence that validates the safety of Li-ESWT for treating CP/CPPS.

AUTHOR CONTRIBUTIONS

YRW and BF conceived the study, drafted the manuscript, and provided statistical expertise. WBQ, YWG, XBK, and HC provided technical assistance. ZLD, JQT, and ZPW critically revised the manuscript. ZPW participated in the study design and manuscript revision. All authors read and approved the final manuscript.

COMPETING INTEREST

All authors declare no competing interests.

ACKNOWLEDGMENT

This work was supported by grants from the National Natural Science Foundation of China (No. PR0121015), the National Natural Science Foundation of China (No. 82160148), and the Natural Science Foundation Project of Gansu Province (No. 2106RJZA110).

Supplementary Information is linked to the online version of the paper on the *Asian Journal of Andrology* website.

REFERENCES

1 Chaussy C, Brendel W, Schmiedt E. Extracorporeally induced destruction of kidney stones by shock waves. *Lancet* 1980; 316: 1265–68.
2 Shrivastava SK, Kailash. Shock wave treatment in medicine. *J Biosci* 2005; 30: 269–75.
3 Müller A, Akin-Olugbade Y, Deveci S, Donohue JF, Tal R, *et al*. The impact of shock wave therapy at varied energy and dose levels on functional and structural changes in erectile tissue. *Eur Urol* 2008; 53: 635–43.
4 Vardi Y, Appel B, Jacob G, Massarwi O, Gruenwald I. Effect of low-energy linear shockwave therapy on erectile dysfunction-a double-blinded, sham-controlled,

randomized clinical trial. *Eur Urol* 2010; 58: 243–48.
5 Fojecki GL, Tiessen S, Osther PJ. Effect of low-energy linear shockwave therapy on erectile dysfunction-a double-blinded, sham-controlled, randomized clinical trial. *J Sex Med* 2017; 14: 106–12.
6 Wuerfel T, Schmitz C, Jokinen LL. The effects of the exposure of musculoskeletal tissue to extracorporeal shock waves. *Biomedicines* 2022; 10: 1084.
7 Antonic V, Mittermayr R, Schaden W, Stojadinovic A. Evidence supporting extracorporeal shock wave therapy for acute and chronic soft tissue wounds. *Wounds* 2011; 23: 204–15.
8 Liu Z, Murphy SF, Wong L, Schaeffer AJ, Thumbikat P. Neuronal/astrocytic expression of chemokine (C-C motif) ligand 2 is associated with monocyte/macrophage recruitment in male chronic pelvic pain. *Pain* 2020; 161: 2581–91.
9 Engeler DS, Baranowski AP, Dinis-Oliveira P, Elneil S, Hughes J, *et al*. The 2013 EAU guidelines on chronic pelvic pain: is management of chronic pelvic pain a habit, a philosophy, or a science? 10 years of development. *Eur Urol* 2013; 64: 431–9.
10 Franco JV, Turk T, Jung JH, Xiao YT, Iakhno S, *et al*. Pharmacological interventions for treating chronic prostatitis/chronic pelvic pain syndrome. *Cochrane Database Syst Rev* 2018; 1: CD012551.
11 Clemens JQ, Mullins C, Ackerman AL, Bavendam T, van Bokhoven A, *et al*. Urologic chronic pelvic pain syndrome: insights from the MAPP research network. *Nat Rev Urol* 2019; 16: 187–200.
12 Zimmermann R, Cumpanas A, Hoeltl L, Janetschek G, Stenzl A, *et al*. Extracorporeal shock-wave therapy for treating chronic pelvic pain syndrome: a feasibility study and the first clinical results. *BJU Int* 2008; 102: 976–80.
13 Kong X, Hu W, Dong Z, Tian J, Wang Y, *et al*. The efficacy and safety of low-intensity extracorporeal shock wave treatment combined with or without medications in chronic prostatitis/chronic pelvic pain syndrome: a systematic review and meta-analysis. *Prostate Cancer Prostatic Dis* 2023; 26: 483–94.
14 Manfredi C, Arcaniolo D, Amicuzi U, Spirito L, Napolitano L, *et al*. Impact of extracorporeal shockwave therapy for erectile dysfunction and Peyronie's disease on reproductive and hormonal testicular function. *Andrology* 2022; 10: 1368–75.
15 Krieger JR, Rizk PJ, Kohn TP, Pastuszak A. Shockwave therapy in the treatment of Peyronie's disease. *Sex Med Rev* 2019; 7: 499–507.
16 Porst H. Review of the current status of low intensity extracorporeal shockwave therapy (Li-ESWT) in erectile dysfunction (ED), Peyronie's disease (PD), and sexual rehabilitation after radical prostatectomy with special focus on technical aspects of the different marketed ESWT devices including personal experiences in 350 patients. *Sex Med Rev* 2021; 9: 93–122.
17 Feng B, Dong Z, Wang Y, Yan G, Yang E, *et al*. Li-ESWT treatment reduces inflammation, oxidative stress, and pain via the PI3K/AKT/FOXO1 pathway in autoimmune prostatitis rat models. *Andrology* 2021; 9: 1593–602.
18 Zang ZJ, Liu Q, Hu J, Feng J, Zhu YQ, *et al*. The impact of low-intensity extracorporeal shock wave therapy on testicular function in adult rats. *Andrology* 2018; 6: 936–42.
19 de Bono JS, Guo C, Gurel B, De Marzo AM, Sfanos KS, *et al*. Prostate carcinogenesis: inflammatory storms. *Nat Rev Cancer* 2020; 20: 455–69.
20 Elkahwaji JE, Hauke RJ, Brawner CM. Chronic bacterial inflammation induces prostatic intraepithelial neoplasia in mouse prostate. *Br J Cancer* 2009; 101: 1740–8.
21 Elkahwaji JE, Zhong W, Hopkins WJ, Bushman W. Chronic bacterial infection and inflammation incite reactive hyperplasia in a mouse model of chronic prostatitis. *Prostate* 2007; 67: 14–21.
22 Rola P, Włodarczak A, Barycki M, Doroszko A. Use of the shock wave therapy in basic research and clinical applications-from bench to bedsite. *Biomedicines* 2022; 10: 3.
23 Mykoniatis I, Pyrgidis N, Kalyvianakis D, Zilotis F, Kapoteli P, *et al*. Comparing two different low-intensity shockwave therapy frequency protocols for nonbacterial chronic prostatitis/chronic pelvic pain syndrome: a two-arm, parallel-group randomized controlled trial. *Prostate* 2021; 81: 499–507.
24 Daneshwar D, Nordin A. Treatment of prostatitis with low-intensity extracorporeal shockwave therapy (LI-ESWT). *Int Urol Nephrol* 2023; 55: 3133–45.
25 Sokmen D, Comez YI. Long-term efficacy and safety of extracorporeal shock wave therapy (Li-ESWT) protocols in the treatment of chronic prostatitis/chronic pelvic pain syndrome (CP/CPPS) patients. *Aging Male* 2023; 26: 2253876.
26 Skaudickas D, Lenčiauskas P, Skaudickas A, Undžytė G. Low intensity extracorporeal shockwave therapy for chronic pelvic pain syndrome: long-term follow-up. *Open Med (Wars)* 2023; 18: 20230832.
27 Ohl CD, Wolfrum B. Detachment and sonoporation of adherent HeLa-cells by shock wave-induced cavitation. *Biochim Biophys Acta* 2003; 1624: 131–8.
28 Webber MM, Quader ST, Kleinman HK, Bello-DeOcampo D, Storto PD, *et al*. Human cell lines as an *in vitro in vivo* / model for prostate carcinogenesis and progression. *Prostate* 2001; 47: 1–13.
29 Rhim JS. Molecular and genetic mechanisms of prostate cancer. *Radiat Res* 2001; 155: 128–32.
30 Fontana F, Anselmi M, Limonta P. Molecular mechanisms and genetic alterations in prostate cancer: from diagnosis to targeted therapy. *Cancer Lett* 2022; 534: 215619.
31 Kulkarni P, Dasgupta P, Bhat NS, Hashimoto Y, Saini S, *et al*. Role of the PI3K/Akt pathway in cadmium induced malignant transformation of normal prostate epithelial cells. *Toxicol Appl Pharm* 2020; 409: 115308.
32 Allott EH, Masko EM, Freedland SJ. Obesity and prostate cancer: weighing the evidence. *Eur Urol* 2013; 63: 800–9.
33 Kuettel MR, Thraves PJ, Jung M, Varghese SP, Prasad SC, *et al*. Radiation-induced neoplastic transformation of human prostate epithelial cells. *Cancer Res* 1996; 56: 5–10.
34 Rhim JS, Jin S, Jung M, Thraves PJ, Kuettel MR, *et al*. Malignant transformation of human prostate epithelial cells by N-nitroso-N-methylurea. *Cancer Res* 1997; 57: 576–80.
35 Nakamura K, Yasunaga Y, Ko D, Xu LL, Moul JW, *et al*. Cadmium-induced neoplastic transformation of human prostate epithelial cells. *Int J Oncol* 2002; 20: 543–7.
36 Takahashi T, Nakagawa K, Tada S, Tsukamoto A. Low-energy shock waves evoke intracellular Ca^{2+} increases independently of sonoporation. *Sci Rep* 2019; 9: 3218.
37 Liu T, Shindel AW, Lin G, Lue TF. Cellular signaling pathways modulated by low-intensity extracorporeal shock wave therapy. *Int J Impot Res* 2019; 31: 170–6.
38 Zhang B, Fu D, Xu Q, Cong X, Wu C, *et al*. The senescence-associated secretory phenotype is potentiated by feedforward regulatory mechanisms involving Zscan4 and TAK1. *Nat Commun* 2018; 9: 1723.
39 Wiseman H, Halliwell B. Damage to DNA by reactive oxygen and nitrogen species: role in inflammatory disease and progression to cancer. *Biochem J* 1996; 313: 17–29.
40 Eiserich JP, Hristova M, Cross CE, Jones AD, Freeman BA, *et al*. Formation of nitric oxide-derived inflammatory oxidants by myeloperoxidase in neutrophils. *Nature* 1998; 391: 393–7.
41 Lehmann BD, Paine MS, Brooks AM, McCubrey JA, Renegar RH, *et al*. Senescence-associated exosome release from human prostate cancer cells. *Cancer Res* 2008; 68: 7864–71.
42 d'Agostino MC, Craig K, Tibalt E, Respizzi S. Shock wave as biological therapeutic tool: from mechanical stimulation to recovery and healing, through mechanotransduction. *Int J Surg* 2015; 24: 147–53.
43 Schuh C, Heher P, Weihs AM, Banerjee A, Fuchs C, *et al*. *In vitro* extracorporeal shock wave treatment enhances stemness and preserves multipotency of rat and human adipose-derived stem cells. *Cytotherapy* 2014; 16: 1666–78.
44 Wang W, Prokopec JS, Zhang Y, Sukhoplyasova M, Shinglot H, *et al*. Sensing plasma membrane pore formation induces chemokine production in survivors of regulated necrosis. *Dev Cell* 2022; 57: 228–45.e6.
45 Barnes JL, Zubair M, John K, Poirier MC, Martin FL. Carcinogens and DNA damage. *Biochem Soc Trans* 2018; 46: 1213–24.
46 Liu Y, Chen X, Guo A, Liu S, Hu G. Quantitative assessments of mechanical responses upon radial extracorporeal shock wave therapy. *Adv Sci (Weinh)* 2018; 5: 1700797.
47 Juríková M, Danihel Ľ, Polák Š, Varga I. Ki67, PCNA, and MCM proteins: markers of proliferation in the diagnosis of breast cancer. *Acta Histochem* 2016; 118: 544–52.
48 Cui K, Kang N, Banie L, Zhou T, Liu T, *et al*. Microenergy acoustic pulses induced myogenesis of urethral striated muscle stem/progenitor cells. *Transl Androl Urol* 2019; 8: 489–500.
49 Peng D, Reed-Maldonado AB, Zhou F, Tan Y, Yuan H, *et al*. Exosome released from Schwann cells may be involved in microenergy acoustic pulse-associated cavernous nerve regeneration. *J Sex Med* 2020; 17: 1618–28.
50 Wang HS, Ruan Y, Banie L, Cui K, Kang N, *et al*. Delayed low-intensity extracorporeal shock wave therapy ameliorates impaired penile hemodynamics in rats subjected to pelvic neurovascular injury. *J Sex Med* 2019; 16: 17–26.
51 Huang N, Qin Z, Sun W, Bao K, Zha J, *et al*. Comparing the effectiveness of extracorporeal shockwave therapy and myofascial release therapy in chronic pelvic pain syndrome: study protocol for a randomized controlled trial. *Trials* 2023; 24: 675.
52 Zhang ZX, Zhang D, Yu XT, Ma YW. Efficacy of radial extracorporeal shock wave therapy for chronic pelvic pain syndrome: a nonrandomized controlled trial. *Am J Mens Health* 2019; 13: 155798831881466.
53 Rayegani SM, Razzaghi MR, Raeissadat SA, Allameh F, Eliaspour D, *et al*. Extracorporeal shockwave therapy combined with drug therapy in chronic pelvic pain syndrome – a randomized clinical trial. *Urol J* 2020; 17: 185–91.
54 Verze P, Cai T, Lorenzetti S. The role of the prostate in male fertility, health and disease. *Nat Rev Urol* 2016; 13: 379–86.
55 Di X, Gao X, Peng L, Ai J, Jin X, *et al*. Cellular mechanotransduction in health and diseases: from molecular mechanism to therapeutic targets. *Sig Transduct Target Ther* 2023; 8: 282.

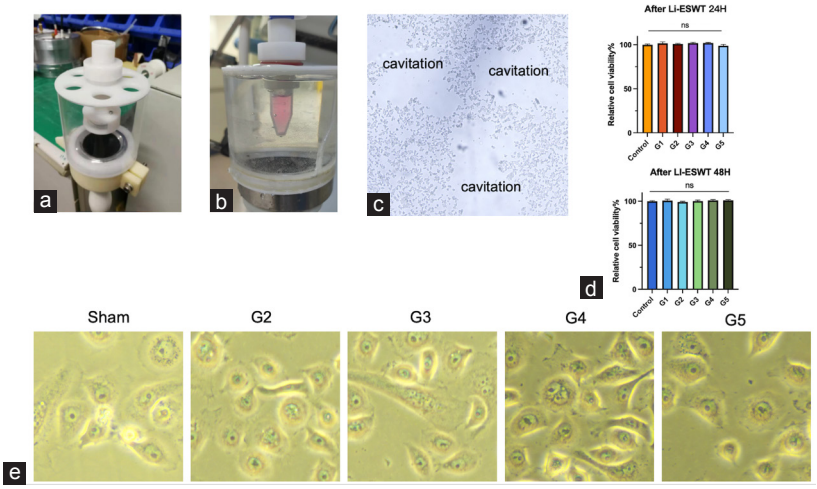

Supplementary Figure 1: (**a**) Li-ESWT adherent cell *in vitro* model. (**b**) Li-ESWT nonadherent cell *in vitro* model. (**c**) Cavitation effect in the adherent cell *in vitro* model. (**d**) CCK-8 assay results of RWPE-1 cells exposed to different Li-ESWT levels in the adherent cell *in vitro* model. (**e**) Representative images of the RWPE-1 *in vitro* cell model and the sham group exposed to Li-ESWT (×20). CCK-8: Cell Counting Kit-8; Li-ESWT: low-intensity extracorporeal shock wave.

Supplementary Table 1: Physical parameters of extracorporeal shock wave therapy *in vitro* culture model

Calibration energy level	*Physical parameters of ESWT in vitro culture model*			
	Cell culture dish (35 mm)		*Centrifuge tube (15 ml)*	
	Energy flux density (mJ mm^{-2})	*Peak sound pressure (Mpa)*	*Energy flux density (mJ mm^{-2})*	*Peak sound pressure (Mpa)*
1	0.04	10.4	0.05	10.4
2	0.06	11.6	0.03	7.8
3	0.09	13.1	0.05	9.5
4	0.12	16.3	0.03	9.2
5	0.16	18.5	0.09	12.2

ESWT: extracorporeal shock wave therapy

Supplementary Table 2: Single-nucleotide polymorphism and insertion–deletions number of control group and extracorporeal shock wave therapy group

Sample name	*SNP number*	*InDel number*
LiESWT-1	43773	3924
LiESWT-2	43647	3824
LiESWT-3	43689	3903
RWPE1-1	43771	3951
RWPE1-2	43790	3948
RWPE1-3	43699	3896

SNP: single-nucleotide polymorphism; InDel: insertion–deletions; LiESWT: low intensity extracorporeal shock wave therapy; RWPE1: prostate epithelial